

THE EFFECT OF THE TRANSVERSE BEAM JITTER ON THE ACCELERATED ELECTRON BEAM QUALITY IN A LASER-DRIVEN PLASMA ACCELERATOR WITH EXTERNAL INJECTION AT SINBAD FOR ATHENA_e

E. N. Svystun[†], R. W. Assmann, U. Dorda, B. Marchetti, Deutsches Elektronen-Synchrotron, DESY, 22607 Hamburg, Germany

Abstract

Laser plasma accelerators with external injection of an RF-generated electron beam, providing high accelerating field gradients and increased control over the electron beam injection process, are promising candidates for producing electron beams matching the requirements of modern user-applications. Experiments in this field are planned at the SINBAD (Short INnovative Bunches and Accelerators at DESY) facility in the context of the ATHENA_e (Accelerator Technology HELmholtz iNfrAstructure) project. In this paper we present numerical studies on the effect of the transverse electron beam jitter on the final quality of a sub-femtosecond, 0.8 pC, 100 MeV electron beam accelerated to 1 GeV energy in the plasma wakefield driven by a 196 TW, 5 J laser pulse.

INTRODUCTION

Laser-driven plasma wakefield acceleration (LWFA) offers the possibility to accelerate charged particles with average acceleration gradients of the order of GV/m [1]. Successful experiments of LWFA have confirmed the relevance of this acceleration technology through the demonstration of GeV-class electron beam generation [2]. However, to prove the potential of laser-plasma accelerators (LPAs) to be the next-generation compact sources for the production of high-energy beams, the quality and stability of the plasma-generated electron beams need to be improved. One promising candidate to meet the requirements of modern applications on the accelerated beam quality is LPA with external injection of an electron beam produced by an RF linac. On the one hand, this acceleration scheme is promising as it allows good control of the input beam parameters. On the other hand, this approach is interesting as it could allow the experimental setup to be extended to a multistage LPA with potential applications for future high-energy colliders.

LWFA with external injection are the baseline experiments foreseen at SINBAD [3] within the framework of ATHENA_e. They will focus on controlled injection, acceleration and extraction from the plasma of electron beams generated by a normal-conducting 100 MeV S-band ARES (Accelerator Research Experiment at Sinbad) linear accelerator [4].

ATHENA is a strategic research and development project structured into two technology flagship projects, dedi-

cated to electron acceleration (ATHENA_e) and hadron acceleration (ATHENA_h), and several application projects. The flagship project ATHENA_e will be hosted at the SINBAD facility at DESY. The goal of the ATHENA infrastructure is to demonstrate for the first time user-relevant applications of laser plasma accelerators, opening the door to new, cost effective accelerator applications in science, hospitals and industry.

RESULTS AND DISCUSSION

The following parameters regarding the potential experimental setup for LWFA with external injection at SINBAD for ATHENA_e were numerically studied and justified in [5], in order to optimize the beam quality during acceleration and extraction processes:

- the transverse plasma density profile;
- the longitudinal plasma density profile (up- and down-ramps);
- the length of the plasma acceleration region.

In this paper we extend the numerical studies reported in [5], in order to investigate the effect of the transverse beam jitter on the accelerated electron beam quality in an LPA with external injection at SINBAD for ATHENA_e.

The three-dimensional start-to-end simulations have been carried out with the spectral quasi-cylindrical particle-in-cell (PIC) code FBPIC [6]. The dimensions of the copropagating simulation window in the longitudinal and transverse directions are $118 \times 420 \mu\text{m}^2$ with a resolution of $0.022 \times 0.5 \mu\text{m}^2$. The time step is 74 as, corresponding to a length of 22.19 nm. A third order particle shape function and 8 particles per cell are used for the plasma. The total number of beam particles is equal to 158280. The simulations were run in a Lorentz boosted frame with a frame relativistic factor of $\gamma_f = 5$. The Galilean-Pseudo-spectral analytical time-domain (Galilean-PSATD) solver [7, 8] has been used for electromagnetic field calculations to eliminate the numerical Cherenkov instability (NCI) [9, 10].

The following laser pulse parameters were assumed: pulse length $\tau_l = 25$ fs (FWHM); spot size $w_0 = 42.47 \mu\text{m}$; peak normalized vector potential $a_0 = 1.8$; peak power $P_L = 196$ TW, wavelength $\lambda_l = 800$ nm. The laser transverse and temporal profiles are Gaussian. The laser pulse and the electron beam are injected collinearly into a plasma channel with a radially parabolic density profile of the form $n(r) = n_0 + \Delta n(r/r_{ch})^2$, where the channel depth $\Delta n = 0.626n_0$, the channel width $r_{ch} = 42.47 \mu\text{m}$ and the on-axis plasma density $n_0 = 1 \times 10^{17} \text{cm}^{-3}$. The plasma wavelength is $\lambda_p = 106 \mu\text{m}$ and the plasma skin depth is $c/\omega_p = k_p^{-1} = 16.8 \mu\text{m}$, with the plasma frequency given by

[†] email address: elena.svystun@desy.de

$\omega_p = (n_0 e^2 / \epsilon_0 m_e)^{1/2}$, where c is the speed of light, k_p is the plasma wave number, e is the electron charge, ϵ_0 is the vacuum permittivity and m_e is the electron mass.

The following longitudinal plasma density profile was implemented in all simulations to match an electron beam into the plasma focusing field and thus to control the emittance growth of the beam in the plasma section [11]:

$$f(z) = \frac{1}{(1 \mp (z - z_{0,u/d})/l_{u/d})^2}. \quad (1)$$

Here $z_{0,u}$ and $z_{0,d}$ are the longitudinal coordinates of the start of the up-ramp and the down-ramp respectively; l_u and l_d are the optimized characteristic scale lengths of the plasma adiabatic matching sections given by:

$$l_{u/d} = \beta_{p0} \sqrt{\left(\frac{(N+1)\pi}{\ln(\beta_{i|goal}/\beta_{goal|i})} \right)^2 + \frac{1}{4}}, \quad (2)$$

where β_{p0} is the beta function of the matched electron beam in PBAs, $\beta_{p0} = \sqrt{\gamma_b c m_e / (g e)}$, with γ_b being the beam Lorentz factor and g being the transverse focusing field in the plasma; $N = 0, 1, 2, \dots$; β_i is the initial beta function of the beam; β_{goal} is the beta function of the beam matched to the plasma section in the case of the plasma up-ramp and to the external focusing elements in the case of the down-ramp. The lengths of the plasma up-ramp and down-ramp are then given by

$$L_{u/d} = (\beta_{i|goal}/\beta_{goal|i} - 1)l_{u/d} \quad (3)$$

In all simulations the length of the plasma up-ramp is equal to 0.6 cm and the length of the down-ramp is equal to 0.9 cm. The length of the acceleration region is equal to 9.5 cm. The laser pulse is focused into the plasma after the end of the plasma up-ramp.

A full set of initial parameters of the ARES electron beam considered in this paper is given in Table 1. The beam parameters correspond to WP1 in [12] but we have considered 100% of the particles. The following temporal offsets between the electron beam center and the peak of the laser pulse envelope $\Delta\tau_{eb/lp}$ were considered: 211.6 fs

Table 1: Electron Beam Parameters at the Plasma Entrance

Charge, Q [pC]	0.8
Peak current, I_{peak} [kA]	0.55
Mean energy, \bar{E} [MeV]	100
Relative energy spread, $\Delta E/\bar{E}$ [%]	0.2
Longitudinal RMS size, $\sigma_{z,rms}$ [μm]	0.155 (0.5 fs)
Horizontal RMS size, $\sigma_{x,rms}$ [μm]	0.80
Vertical RMS size, $\sigma_{y,rms}$ [μm]	0.73
Normalized horizontal emittance, $\epsilon_{n,x}$ [μm]	0.11
Normalized vertical emittance, $\epsilon_{n,y}$ [μm]	0.10
Beta-functions, β_x/β_y [mm]	1.13 / 1.0
Beam density, n_b [cm^{-3}]	34.6×10^{17}

(63.4 μm), 193.8 fs (58.1 μm) and 176 fs (52.8 μm). A temporal electron beam-laser offset of 211.6 fs corresponds to the case when the external beam is injected near the on-crest acceleration phase, at the position of maximum accelerating field amplitude.

Four cases for the beam displacement and divergence at the injection point were defined based on [4] to investigate the effect of the transverse beam jitter on the accelerated electron beam quality. The simulations in [4] have been done considering a lattice matching the electron beam to the plasma without any constraints coming from the integration of the incoupling optics for the high-power laser. The position and pointing jitters of the beam are caused by the transverse jitter of the laser on the photo-cathode, which in this case was assumed to be of the order of 20 μm RMS. In case 1, the initial beam is displaced in the positive direction and offset by:

$$\begin{aligned} \Delta x &= 0.2 \mu\text{m} (0.25 \sigma_{x,rms}), & \Delta y &= 1 \mu\text{m} (1.37 \sigma_{y,rms}), \\ \Delta x' &= -150 \mu\text{rad}, & \Delta y' &= +400 \mu\text{rad}, \end{aligned} \quad (4)$$

where Δx and Δy are the positional displacements (offsets) of the beam at the injection point in x and y respectively, and $\Delta x'$ and $\Delta y'$ are the angular offsets in x' and y' respectively.

In case 2, the initial beam is displaced in the negative direction and offset by:

$$\begin{aligned} \Delta x &= -0.15 \mu\text{m} (0.19 \sigma_{x,rms}), & \Delta y &= -1 \mu\text{m} (1.37 \sigma_{y,rms}), \\ \Delta x' &= +160 \mu\text{rad}, & \Delta y' &= -400 \mu\text{rad}. \end{aligned} \quad (5)$$

In case 3, the initial beam is displaced in the positive direction and offset by

$$\begin{aligned} \Delta x &= 0.4 \mu\text{m} (0.5 \sigma_{x,rms}), & \Delta y &= 2 \mu\text{m} (2.74 \sigma_{y,rms}), \\ \Delta x' &= -300 \mu\text{rad}, & \Delta y' &= +800 \mu\text{rad}. \end{aligned} \quad (6)$$

In case 4, the initial beam is displaced in the negative direction and offset by

$$\begin{aligned} \Delta x &= -0.3 \mu\text{m} (0.38 \sigma_{x,rms}), & \Delta y &= -2 \mu\text{m} (2.74 \sigma_{y,rms}), \\ \Delta x' &= +320 \mu\text{rad}, & \Delta y' &= -800 \mu\text{rad}. \end{aligned} \quad (7)$$

The results of the three-dimensional start-to-end simulations are summarized in Table 2, 3 and 4.

A small longitudinal RMS size (the beam occupies a tiny fraction of the plasma wave length, $\sigma_{z,rms} \approx 0.0015 \lambda_p$) and injection of the beam at a suitable phase of the exited plasma wave allows the growth of the beam relative energy spread during the acceleration process to be mitigated. Depending on the injection phase, the relative energy spread of the beam can even be reduced during the acceleration process (see Tables 1 and 3). For the considered parameter set, the evolution of the relative energy spread of the accelerated beam is described in detail in [5].

Table 2: Parameters of the Accelerated Electron Beam after Extraction from the Plasma in a Case of Electron Beam-Laser Temporal Offset of $\Delta\tau_{eb/lp} = 211.6$ fs

Displacement case	w/o	1	2	3	4
I_{peak} [kA]	0.55	0.55	0.55	0.55	0.55
\bar{E} [MeV]	1143	1142.7	1142.6	1142	1142
$\Delta E/\bar{E}$ [%]	0.27	0.28	0.29	0.30	0.30
$\sigma_{z,rms}$ [μm]	0.17	0.17	0.17	0.17	0.17
$\sigma_{x,rms}$ [μm]	0.70	0.70	0.70	0.70	0.70
$\sigma_{y,rms}$ [μm]	0.57	0.58	0.58	0.58	0.58
$\varepsilon_{n,x}$ [μm]	0.11	0.11	0.11	0.11	0.11
$\varepsilon_{n,y}$ [μm]	0.10	0.10	0.10	0.10	0.10

Table 3: Parameters of the Accelerated Electron Beam after Extraction from the Plasma in a Case of Electron Beam-Laser Temporal Offset of $\Delta\tau_{eb/lp} = 193.8$ fs

Displacement case	w/o	1	2	3	4
I_{peak} [kA]	0.55	0.55	0.55	0.55	0.55
\bar{E} [MeV]	1065	1065	1065	1064.5	1064.5
$\Delta E/\bar{E}$ [%]	0.16	0.17	0.17	0.18	0.18
$\sigma_{z,rms}$ [μm]	0.17	0.17	0.17	0.17	0.17
$\sigma_{x,rms}$ [μm]	1.07	1.08	1.00	1.00	1.00
$\sigma_{y,rms}$ [μm]	0.90	0.90	0.90	0.90	0.90
$\varepsilon_{n,x}$ [μm]	0.11	0.11	0.11	0.11	0.11
$\varepsilon_{n,y}$ [μm]	0.10	0.10	0.10	0.10	0.10

Table 4: Parameters of the Accelerated Electron Beam after Extraction from the Plasma in a Case of Electron Beam-Laser Temporal Offset of $\Delta\tau_{eb/lp} = 176$ fs

Displacement case	w/o	1	2	3	4
I_{peak} [kA]	0.55	0.55	0.55	0.55	0.55
\bar{E} [MeV]	925	925	924.7	924.6	924.6
$\Delta E/\bar{E}$ [%]	0.29	0.29	0.29	0.29	0.28
$\sigma_{z,rms}$ [μm]	0.17	0.17	0.17	0.17	0.17
$\sigma_{x,rms}$ [μm]	1.45	1.46	1.45	1.47	1.46
$\sigma_{y,rms}$ [μm]	1.24	1.25	1.25	1.27	1.27
$\varepsilon_{n,x}$ [μm]	0.11	0.11	0.11	0.11	0.11
$\varepsilon_{n,y}$ [μm]	0.10	0.10	0.10	0.10	0.10

Plasma density ramps can be used to preserve the beam emittance and control the beam divergence during beam propagation through the plasma channel [11, 13]. In all studied cases of the beam displacement (up to 2 μm) and divergence (up to 800 μrad) at the injection point, the use of the short adiabatic matching sections ($L_u = 0.6$ cm and $L_d = 0.9$ cm) and the low energy spread of the beam allow the beam normalized horizontal and vertical emittances to be conserved during the injection, acceleration and extraction processes (see Tables 1 – 4).

The current distribution, as well as the longitudinal and transverse phase-spaces of the accelerated electron beam after its extraction from the plasma for an electron beam-laser temporal offset of $\Delta\tau_{eb/lp} = 193.8$ fs and case 3 of extreme beam positional and angular offsets are presented in Fig. 1.

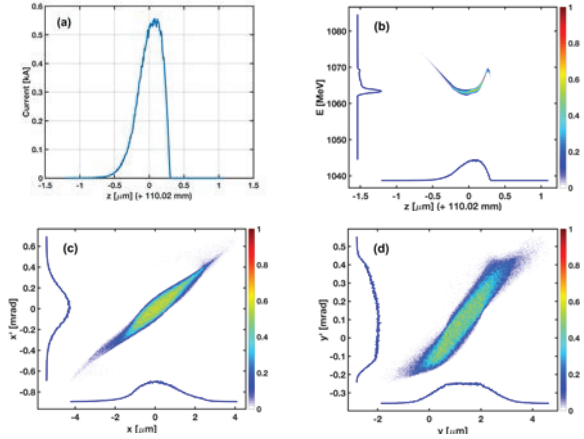


Figure 1: Current distribution (a), longitudinal (b), horizontal (c) and vertical (d) phase-spaces of the accelerated electron beam after its extraction from the plasma target. The electron beam-laser temporal offset is $\Delta\tau_{eb/lp} = 193.8$ fs. Beam displacement and divergence follows case 3. The colormap describes normalized charge.

Studies on the effect of the transverse electron beam jitter on the accelerated beam quality for a potential experimental setup at SINBAD, proposed in [5] for LWFA with external injection, show that tolerances in position and angle of up to 2 μm and 800 μrad respectively, and electron beam-laser synchronization jitter of up to 35.6 fs allow operation in a stable regime. In this regime, the transverse normalized emittances are preserved in both directions throughout the beam acceleration process to GeV energy and are equal to 0.1 μm each, while the final relative energy spread varies from 0.16 up to 0.3 %, depending on the transverse tolerances and electron beam-laser arrival-time jitter.

CONCLUSIONS

Transverse and longitudinal tolerances were studied for a potential experimental setup for laser-driven plasma acceleration with external injection of an electron beam from an RF linac at SINBAD for ATHENA_e through three-dimensional start-to-end PIC simulations. Tolerances in position and angle of up to 2 μm and 800 μrad respectively, and electron beam-laser synchronization jitter of up to 35.6 fs allow a stable regime of operation with quality-preserving acceleration. An iteration on the effect of the tolerances will be needed, after which the technical design of the matching region to the plasma will be completed and updated values for the position and pointing jitters at the entrance of the plasma experiment will be available.

Any distribution of this work must maintain attribution to the author(s), title of the work, publisher, and DOI (© 2019). Content from this work may be used under the terms of the CC BY 3.0 licence (© 2019).

ACKNOWLEDGEMENTS

The authors would like to acknowledge the FBPIC developers and contributors.

REFERENCES

- [1] P. Chen, J.M. Dawson, R.W. Huf, and T. Katsouleas, "Acceleration of Electrons by the Interaction of a Bunched Electron Beam with a Plasma", *Phys. Rev. Lett.*, vol. 54, p. 693, 1985.
- [2] W.P. Leemans, A.J. Gonsalves, H.-S. Mao et al., "Multi-GeV Electron Beams from Capillary-Discharge-Guided Subpetawatt Laser Pulses in the Self-Trapping Regime", *Phys. Rev. Lett.*, vol. 113, p. 245002, 2014; A. J. Gonsalves et al., "Petawatt Laser Guiding and Electron Beam Acceleration to 8 GeV in a Laser-Heated Capillary Discharge Waveguide", *Phys. Rev. Lett.*, vol. 122, p. 084801, 2019.
- [3] U. Dorda *et al.*, "The Dedicated Accelerator R&D Facility Sinbad at DESY", in *Proc. IPAC'17*, Copenhagen, Denmark, May 2017, pp. 869-872.
doi:10.18429/JACoW-IPAC2017-M0PVA012
- [4] B. Marchetti *et al.*, "Conceptual and Technical Design Aspects of Accelerators for External Injection in LWFA", *Appl. Sci.*, vol. 8, no. 5, p. 757, 2018.
<https://doi.org/10.3390/app8050757>
- [5] E.N. Svystun *et al.*, "Numerical studies on electron beam quality optimization in a laser-driven plasma accelerator with external injection at SINBAD for ATHENAe", presented at the 10th Int. Particle Accelerator Conf. (IPAC'19), Melbourne, Australia, May 2019, paper THPGW023, this conference.
- [6] M. Kirchen *et al.*, "Stable discrete representation of relativistically drifting plasmas", *Phys. Plasmas*, vol. 23, p. 100704, 2016.
<https://doi.org/10.1063/1.4964770>
- [7] M. Kirchen *et al.*, "Stable discrete representation of relativistically drifting plasmas", *Phys. Plasmas*, vol. 23, p. 100704, 2016.
<https://doi.org/10.1063/1.4964770>
- [8] R. Lehe *et al.*, "Elimination of Numerical Cherenkov Instability in flowing-plasma Particle-In-Cell simulations by using Galilean coordinates", *Phys. Rev. E*, vol. 94, p. 053305, 2016.
<https://doi.org/10.1103/PhysRevE.94.053305>
- [9] B. B. Godfrey, "Numerical Cherenkov instabilities in electromagnetic particle codes", *J. Comput. Phys.*, vol. 15, pp. 504-521, 1974.
[https://doi.org/10.1016/0021-9991\(74\)90076-X](https://doi.org/10.1016/0021-9991(74)90076-X)
- [10] B. B. Godfrey, "Canonical momenta and numerical instabilities in particle codes", *J. Comput. Phys.*, vol. 19, pp. 58-76, 1975.
[https://doi.org/10.1016/0021-9991\(75\)90116-3](https://doi.org/10.1016/0021-9991(75)90116-3)
- [11] X. L. Xu *et al.*, "Physics of phase space matching for staging plasma and traditional accelerator components using longitudinally tailored plasma profiles", *Phys. Rev. Lett.*, vol. 116, p. 124801, 2016.
- [12] J. Zhu *et al.*, "Lattice design and start-to-end simulations for the ARES linac", *Nucl. Instr. Meth. A*, vol. 909, p. 467, 2018.
<https://doi.org/10.1016/j.nima.2018.02.045>
- [13] K. Floettmann, "Adiabatic matching section for plasma accelerated beams", *Phys. Rev. ST Accel. Beams*, vol. 17, p. 054402, 2014.
<https://doi.org/10.1103/PhysRevSTAB.17.054402>